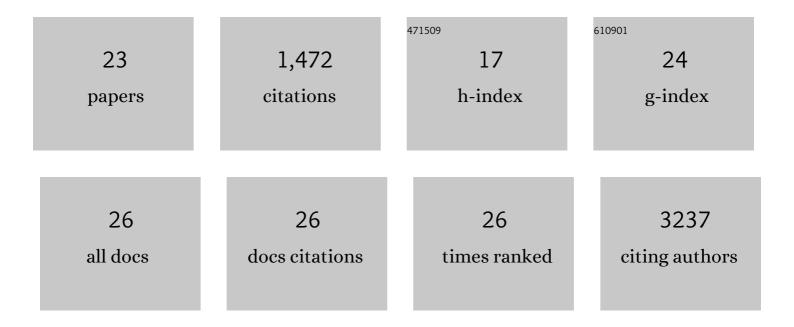
## Véronique Geoffroy

List of Publications by Year in descending order

Source: https://exaly.com/author-pdf/4382393/publications.pdf Version: 2024-02-01



#	Article	IF	CITATIONS
1	AnnotSV: an integrated tool for structural variations annotation. Bioinformatics, 2018, 34, 3572-3574.	4.1	231
2	Efficient strategy for the molecular diagnosis of intellectual disability using targeted high-throughput sequencing. Journal of Medical Genetics, 2014, 51, 724-736.	3.2	229
3	Exome sequencing of Bardet–Biedl syndrome patient identifies a null mutation in the BBSome subunit <i>BBIP1</i> ( <i>BBS18</i> ). Journal of Medical Genetics, 2014, 51, 132-136.	3.2	124
4	Targeted high-throughput sequencing for diagnosis of genetically heterogeneous diseases: efficient mutation detection in Bardet-Biedl and Alström Syndromes. Journal of Medical Genetics, 2012, 49, 502-512.	3.2	104
5	A targeted next-generation sequencing assay for the molecular diagnosis of genetic disorders with orodental involvement. Journal of Medical Genetics, 2016, 53, 98-110.	3.2	100
6	Homozygosity Mapping and Candidate Prioritization Identify Mutations, Missed by Whole-Exome Sequencing, in SMOC2, Causing Major Dental Developmental Defects. American Journal of Human Genetics, 2011, 89, 773-781.	6.2	88
7	VaRank: a simple and powerful tool for ranking genetic variants. PeerJ, 2015, 3, e796.	2.0	80
8	Identification of a novel mutation confirms the implication of IFT172 (BBS20) in Bardet–Biedl syndrome. Journal of Human Genetics, 2016, 61, 447-450.	2.3	64
9	Mutations in TUBGCP4 Alter Microtubule Organization via the γ-Tubulin Ring Complex in Autosomal-Recessive Microcephaly with Chorioretinopathy. American Journal of Human Genetics, 2015, 96, 666-674.	6.2	60
10	Rare De Novo Missense Variants in RNA Helicase DDX6 Cause Intellectual Disability and Dysmorphic Features and Lead to P-Body Defects and RNA Dysregulation. American Journal of Human Genetics, 2019, 105, 509-525.	6.2	50
11	Intragenic FMR1 disease-causing variants: a significant mutational mechanism leading to Fragile-X syndrome. European Journal of Human Genetics, 2017, 25, 423-431.	2.8	48
12	A mutation in VPS15 (PIK3R4) causes a ciliopathy and affects IFT20 release from the cis-Golgi. Nature Communications, 2016, 7, 13586.	12.8	46
13	Proteasome subunit <i>PSMC3</i> variants cause neurosensory syndrome combining deafness and cataract due to proteotoxic stress. EMBO Molecular Medicine, 2020, 12, e11861.	6.9	43
14	Mutations in the latent TGF-beta binding protein 3 (LTBP3) gene cause brachyolmia with amelogenesis imperfecta. Human Molecular Genetics, 2015, 24, 3038-3049.	2.9	40
15	AnnotSV and knotAnnotSV: a web server for human structural variations annotations, ranking and analysis. Nucleic Acids Research, 2021, 49, W21-W28.	14.5	38
16	Identification and Characterization of Known Biallelic Mutations in the IFT27 (BBS19) Gene in a Novel Family With Bardet-Biedl Syndrome. Frontiers in Genetics, 2019, 10, 21.	2.3	30
17	Whole-genome sequencing in patients with ciliopathies uncovers a novel recurrent tandem duplication in <i>IFT140</i> . Human Mutation, 2018, 39, 983-992.	2.5	21
18	A <scp><i>BBS1</i> SVA</scp> F retrotransposon insertion is a frequent cause of <scp>Bardetâ€Biedl</scp> syndrome. Clinical Genetics, 2021, 99, 318-324.	2.0	21

#	Article	IF	CITATIONS
19	Mutations in <i>KARS</i> cause a severe neurological and neurosensory disease with optic neuropathy. Human Mutation, 2019, 40, 1826-1840.	2.5	15
20	A New SLC10A7 Homozygous Missense Mutation Responsible for a Milder Phenotype of Skeletal Dysplasia With Amelogenesis Imperfecta. Frontiers in Genetics, 2019, 10, 504.	2.3	11
21	Detection of a Novel DSPP Mutation by NGS in a Population Isolate in Madagascar. Frontiers in Physiology, 2016, 7, 70.	2.8	10
22	Genetic Evidence Supporting the Role of the Calcium Channel, CACNA1S, in Tooth Cusp and Root Patterning. Frontiers in Physiology, 2018, 9, 1329.	2.8	10
23	Novel <i>IQCE</i> variations confirm its role in postaxial polydactyly and cause ciliary defect phenotype in zebrafish. Human Mutation, 2020, 41, 240-254.	2.5	5